# Stochastic surrogate Hamiltonian

Gil Katz,[1,a)] David Gelman,[2,b)] Mark A. Ratner,[3,c)] and Ronnie Kosloff[1,d)]
[1]*Fritz Haber Research Center for Molecular Dynamics, Hebrew University of Jerusalem, Jerusalem 91904, Israel*
[2]*Department of Biophysics, Albert Einstein College of Medicine, New York, New York 10461, USA*
[3]*Department of Chemistry, Northwestern University, Evanston, Illinois 60208-3113, USA*

(Received 3 April 2008; accepted 27 May 2008; published online 21 July 2008)

The surrogate Hamiltonian is a general scheme to simulate the many body quantum dynamics composed of a primary system coupled to a bath. The method has been based on a representative bath Hamiltonian composed of two-level systems that is able to mimic the true system-bath dynamics up to a prespecified time. The original surrogate Hamiltonian method is limited to short time dynamics since the size of the Hilbert space required to obtain convergence grows exponentially with time. By randomly swapping bath modes with a secondary thermal reservoir, the method can simulate quantum dynamics of the primary system from short times to thermal equilibrium. By averaging a small number of realizations converged values of the system observables are obtained avoiding the exponential increase in resources. The method is demonstrated for the equilibration of a molecular oscillator with a thermal bath. © *2008 American Institute of Physics*. [DOI: 10.1063/1.2946703]

## I. INTRODUCTION

A quantum dynamic process is fully characterized by solving the time-dependent Schrödinger equation. The drawback is that the computational effort for a complete solution scales exponentially with the number of degrees of freedom.[1] As a result converged direct solutions of the quantum dynamics have been obtained for systems with a moderate size Hilbert space of up to $\approx 10^8$ states.[2,3] A useful quantum analysis of many body systems requires approaches that can drastically reduce the scaling of the calculations. The system-bath partition is one of the main venues in this direction. The Hamiltonian generating the dynamics becomes

$$\hat{\mathbf{H}} = \hat{\mathbf{H}}_S \otimes \mathbb{1}_B + \mathbb{1}_S \otimes \hat{\mathbf{H}}_B + \hat{\mathbf{H}}_{SB}, \tag{1}$$

where $\hat{\mathbf{H}}_S$ is the Hamiltonian of the primary system, $\hat{\mathbf{H}}_B$ the bath Hamiltonian, and $\hat{\mathbf{H}}_{SB}$ describes the interaction between system and bath. The reduction in computational complexity is obtained by splitting the representation to a system that requires a full quantum description and a bath described implicitly. The final outcome is equations of motion for relevant dynamics, which are computationally tractable.

The reduced description aims at obtaining equations of motion for the system only. The dynamics of the combined system-bath are generated by the Hamiltonian equation (1) and therefore are unitary. The system dynamics are obtained by tracing out the bath degrees of freedom. As a result the system equations of motion become nonunitary, resulting in equations of motion for the density operator $\hat{\boldsymbol{\rho}}_S$. Formally the dynamics of the reduced density operator $\hat{\boldsymbol{\rho}}_S$ is given by a closed integrodifferential equation,[4,5]

$$\frac{d}{dt}\hat{\boldsymbol{\rho}}_S = \mathcal{L}_S(\hat{\boldsymbol{\rho}}_S) + \int^t \mathcal{K}(t,\tau)\hat{\boldsymbol{\rho}}_S(\tau)d\tau, \tag{2}$$

where $\mathcal{L}_S$ is the system's free Liouville operator and $\mathcal{K}$ is a memory kernel, which includes implicitly the bath dynamics. Although formally exact, the memory kernel can generally not be calculated and further assumptions should be considered. To reduce the complexity, further approximations have to be made. A popular approach is the weak system-bath coupling approximation. The outcome is that the implicit bath influence is encapsulated in bath correlation functions. Supplementing the derivation by Markov approximation (time scale separation between system and bath) leads to semigroup differential equations for the density operator $\hat{\boldsymbol{\rho}}_S$.[6,7]

A conceptual jump is to assume semigroup equations of motion from the start without explicitly describing the reduction process. This approach leads to equations of motion for the system,

$$\frac{d\hat{\boldsymbol{\rho}}_S}{dt} = \mathcal{L}\hat{\boldsymbol{\rho}}_S, \tag{3}$$

where $\mathcal{L}$ is the generator of the semigroup dynamics.[8–10] Based on very general arguments $\mathcal{L}$ has an explicit form that can be employed to model specific dynamical scenarios.[11]

Effective numerical schemes have been developed to solve the resulting time-dependent Liouville von Neumann equation.[12–14] The matrix structure of $\hat{\boldsymbol{\rho}}_S$ limits the applicability to up to three spatial degrees of freedom or a Hilbert space dimension of $\approx 10^4$. When applied to pump-probe-type experiments these methods suffer from a lack of consistency.

[a)]Electronic mail: gkatz@chem.northwestern.edu.
[b)]Electronic mail: davgelman@gmail.com.
[c)]Electronic mail: ratner@chem.northwestern.edu.
[d)]Electronic mail: ronnie@fh.huji.ac.il.

 

First they usually assume a product system-bath initial state $\hat{\boldsymbol{\rho}}_{SB}=\hat{\boldsymbol{\rho}}_S\otimes\hat{\boldsymbol{\rho}}_B$, which is inconsistent with the typical correlated system-bath initial state.[15] Furthermore the time-dependent driving field in a pump probe scenario modifies the reduced description.

To overcome these difficulties an alternative dynamical description, the surrogate Hamiltonian, was introduced.[16–18] The method is based on a representative description of the bath that in the limit of an infinite number of bath modes reproduces the dynamics of the combined system and bath. The approach requires solving the time-dependent Schrödinger equation rather than the Liouville von Neumann equation of the reduced density operator. A major advantage is that simulating systems subject to strong external fields are straightforward and consistent.[17]

A thermal initial state is obtained by averaging many realizations of system-bath wave packets. An effective scheme for generating correlated initial states is carried out by propagating, in imaginary time $\tau=\beta=1/k_BT$, an equal amplitude random phase wave function.[19] The density operator of the system is finally obtained by averaging over the random phases and tracing out the bath. An implementation of the surrogate Hamiltonian method with the multiconfiguration time-dependent Hartree (MCTDH) scheme using a bath of harmonic oscillators has recently been demonstrated.[20]

The drawback of the surrogate Hamiltonian is that it is limited by the scaling of the Hilbert space with the number of effective bath modes. Typical calculations can include 20 bath modes and a two dimensional primary system leading to a Hilbert space size of $\approx 10^9$. Limiting the simultaneous excitation in the bath can increase the bath size up to 100 modes. The main drawback of the finite bath is that the simulation time is limited by the recurrence time of the bath, determined by the bath density of states.

An alternative wave packet based method to describe system-bath dynamics is the stochastic wave packet approach. It has been shown to be formally equivalent to Lindblad dynamics.[21–25] This leads to nonlinear Schrödinger equations driven by stochastic noise. By averaging a large number of realizations $K$, each one with a different realization of the noise, the reduced density operator $\hat{\boldsymbol{\rho}}_S=\lim_{K\to\infty}(1/K)\Sigma_{k=1}^{K}|\phi_k\rangle\langle\phi_k|$ becomes equivalent to the one generated by Lindblad dynamics. The applicability of the method is dependent on the number of realizations required to reach convergence. Experience shows that for small quantum systems $K$ can be very large.

The present study constructs a combination of the surrogate Hamiltonian method supplemented with a stochastic layer mimicking a larger bath. The inspiration for this work emerges from our experience in random phase thermal averaging of the initial state. It was found that a very small number of realizations was required to converge a large system-bath surrogate Hamiltonian.[19] We therefore expect that adding a secondary stochastic bath will eliminate the recurrence, allowing much longer simulations times with reasonable computational resources.

The following scheme (Fig. 1) describes the approach.

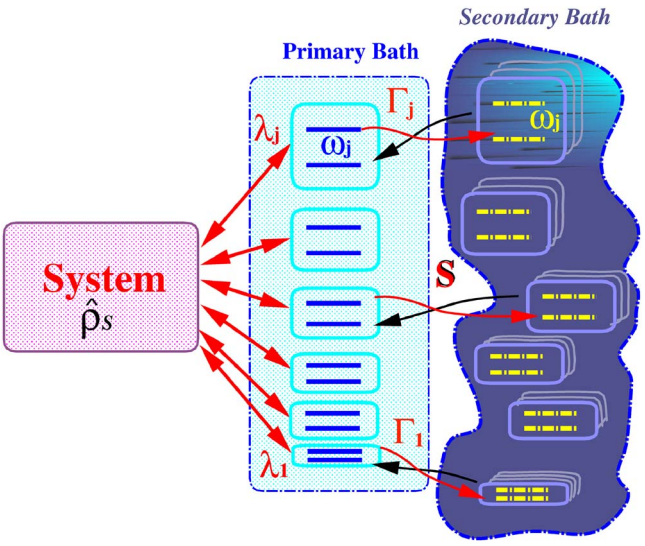


FIG. 1. (Color online) Flowchart of energy currents between the primary system, the primary bath, and the secondary bath. The system and the primary bath are coupled via the Hamiltonian interaction represented by the interaction $\lambda_j$. The primary bath and the secondary bath interact via the swap operation $\hat{\mathbf{S}}$.

## II. STOCHASTIC PROCEDURE

The starting point is dynamics generated by the combined system-bath Hamiltonian,

$$\hat{\mathbf{H}}_T=\hat{\mathbf{H}}_S+\hat{\mathbf{H}}_B+\hat{\mathbf{H}}_{B''}+\hat{\mathbf{H}}_{SB}+\hat{\mathbf{H}}_{BB''}, \tag{4}$$

where $\hat{\mathbf{H}}_S$ represents the system, $\hat{\mathbf{H}}_B$ represents the primary bath, $\hat{\mathbf{H}}_{B''}$ the secondary bath, $\hat{\mathbf{H}}_{SB}$ the system-bath interaction, and $\hat{\mathbf{H}}_{BB''}$ the primary/secondary bath interaction. Formally we trace out the secondary bath and replace it by a stochastic layer. The system and primary bath are represented by the usual surrogate Hamiltonian construction.[17,18,26] We consider the simple version in which the system Hamiltonian takes the form

$$\hat{\mathbf{H}}_S=\hat{\mathbf{T}}+V_S(\hat{\mathbf{R}}), \tag{5}$$

where $\hat{\mathbf{T}}=\hat{\mathbf{P}}^2/2M$ is the kinetic energy operator, $V_S$ is the potential, a function of the system coordinate(s) $\hat{\mathbf{R}}$.

The bath Hamiltonian is composed of a collection of two-level systems,

$$\hat{\mathbf{H}}_B=\sum_j \omega_j\hat{\boldsymbol{\sigma}}_j^{+}\hat{\boldsymbol{\sigma}}_j. \tag{6}$$

The energies $\omega_j$ represent the spectrum of the bath. The system-bath interaction $\hat{\mathbf{H}}_{SB}$ can be chosen to represent different physical processes.[17,18] We will demonstrate the method by an interaction leading to vibrational relaxation,

$$\hat{\mathbf{H}}_{\mathrm{SB}}=\hat{\mathbf{A}}_s\otimes\sum_j^N \lambda_j(\hat{\boldsymbol{\sigma}}_j^{\dagger}+\hat{\boldsymbol{\sigma}}_j), \tag{7}$$

where $\hat{\mathbf{A}}_S$ is the system operator usually chosen as a function of the amplitude $f(\hat{\mathbf{R}}_s)$. $\lambda_j$ is the system-bath coupling parameter of bath mode $j$. When the system-bath coupling is characterized by a spectral density $J(\omega)$ then $\lambda_j=\sqrt{J(\omega_j)/\rho_j}$ and

$\rho_j=(\omega_{j+1}-\omega_j)^{-1}$ are the density of bath modes. We now imagine the secondary bath to be composed of noninteracting two-level systems at temperature $T$ with the same frequency spectrum as the primary bath. At random times a primary and secondary bath modes of the same frequency are swapped.[27] The swap operator $\hat{\mathbf{S}}$ is defined as

$$\hat{\mathbf{S}}\psi_{B_j}\otimes\phi_{B''_j}=\phi_{B_j}\otimes\psi_{B''_j}. \tag{8}$$

In a full swap operation the primary bath mode is reset to a state $\phi$ with thermal amplitudes and random phases,

$$\phi_j=\frac{1}{\sqrt{2\cosh\left[\frac{\hbar\omega_j}{2k_BT}\right]}}\begin{pmatrix}e^{-(\hbar\omega_j/4k_BT)+i\theta_1}\\ e^{+(\hbar\omega_j/4k_BT)+i\theta_2}\end{pmatrix}, \tag{9}$$

where $\theta_1$ and $\theta_2$ are random phases. As a consequence energy is exchanged between the primary and secondary baths at a rate $\kappa_j$ out of mode $j$, $\kappa_j=\Gamma_j\hbar\omega_j(1/2)\coth[\hbar\omega_j/2k_BT]$, where $\Gamma_j$ is the rate of stochastic swaps. The rate $\kappa_j$ should be larger than the rate of energy transfer from the primary system to the primary bath $\Gamma_j\geq\lambda_j$, in order to avoid saturation of the bath modes. When increasing the number of bath modes to obtain convergence, $\lambda_j$ and with it $\Gamma_j$ will decrease with the inverse root of the density of bath modes $1/\sqrt{\rho_j}$. The swap operation has an additional effect of disentangling the system-bath modes. This is not surprising since energy relaxation is always accompanied by dephasing. The ratio $\Gamma_j/\lambda_j$ therefore determines the ratio between the energy relaxation and dephasing rate.

A simple example of the swap operation is as follows: The initial state of the primary system and a bath composed of two modes is

$$\Psi(R_j,a,b)=\psi_1(R_j)a_1b_1+\psi_2(R_j)a_3b_2+\psi_3(R_j)a_2b_1+\psi_4(R_j)a_4b_2, \tag{10}$$

where the vectors $a$ and $b$ represent the amplitude of the bath modes. Bath mode $a$ is swapped with bath mode $c$ of the secondary bath leading to

$$\Psi(R_j,c,b)=\psi_1(R_j)c_1b_1+\psi_2(R_j)c_1b_2+\psi_3(R_j)c_2b_1+\psi_4(R_j)c_2b_2. \tag{11}$$

A more gentle alternative to the above procedure is to use a partial swap operation[27] defined by $\hat{\mathbf{P}}=\hat{\mathbf{I}}\cos\eta+\hat{\mathbf{S}}\sin\eta$. This will cause only a partial reset of each bath mode, maintaining some of the system-bath correlation.

The final state of the system is obtained by taking the partial trace on the combined system-bath density operator obtained by averaging over all the realizations,

$$\hat{\boldsymbol{\rho}}_S=tr_B\left\{\frac{1}{K}\sum_{k=1}^{K}|\Psi_k\rangle\langle\Psi_k|\right\}, \tag{12}$$

where $\Psi_k$ is the combined system-bath wave function with realization $k$. The secondary bath $B'$ appears only implicitly in the state $\Psi_k$ by the number of random swap operation in realization $k$.

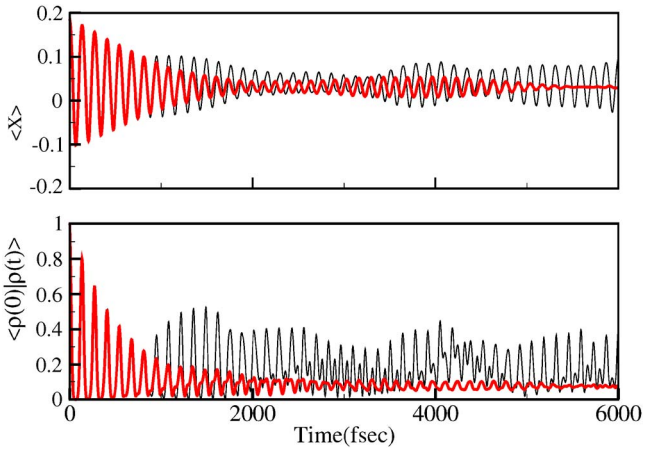


FIG. 2. (Color online) Comparison between the surrogate Hamiltonian (black) and the stochastic surrogate Hamiltonian [red (gray)] is shown. The simulation employed 15 bath modes and 24 realizations. The average position as a function of time is displayed on top and the correlation function on bottom. The initial state is a displaced ground state Morse oscillator state with displacement $R_0=0.1825$ bohr corresponding to Ref. 29. The coupling to bath was adjusted to a relaxation time scale of $1/\gamma_h=1500$ fs.

## III. RESULTS

The method is demonstrated with a system composed of a Morse oscillator coupled to bath. This system has been used before for the comparison of the direct relaxation calculations using MCTDH and semigroup dynamics.[28] In addition the same setup was used to compare a spin bath to a bath composed of harmonic oscillators.[29] The primary system is constructed from an anharmonic (Morse) oscillator of mass $M$,

$$\hat{\mathbf{H}}_S=\frac{\hat{\mathbf{P}}^2}{2M}+D(e^{-2\alpha\hat{\mathbf{R}}}-2e^{-\alpha\hat{\mathbf{R}}}). \tag{13}$$

The coupling term is nonlinear in the Morse oscillator coordinate $R$, but reduces to a linear one for small $R$,

$$f(\hat{\mathbf{R}})=\frac{1-e^{-\alpha\hat{\mathbf{R}}}}{\alpha}. \tag{14}$$

The bath spectral density function was chosen as Ohmic. For this bath the damping rate $\gamma$ is frequency independent. The spectral density in the continuum limit becomes

$$J(\omega)=M\gamma\omega \tag{15}$$

for all frequencies $\omega$ up to the cutoff frequency $\omega_c$. A finite bath with equally spaced sampling of the energy range was used.

The parameters used are the same as in Refs. 28 and 29: a well depth $D$ of 0.018 a.u., $\alpha=2$ bohr$^{-1}$, and a mass of $M=10^5m_e$. For these parameters the number of bond levels becomes $\Lambda\sim29$. The cutoff frequency was chosen as $\omega_c=2.5\ \Omega$, where $\Omega=\alpha^2\sqrt{2D/M}$. All calculations were performed with a total swap operation.

A typical system-bath dynamics is shown in Fig. 2, where the average system position and autocorrelation function are shown. For short times both the standard surrogate Hamiltonian and the stochastic surrogate Hamiltonian follow the same dynamics. At longer time the standard surrogate

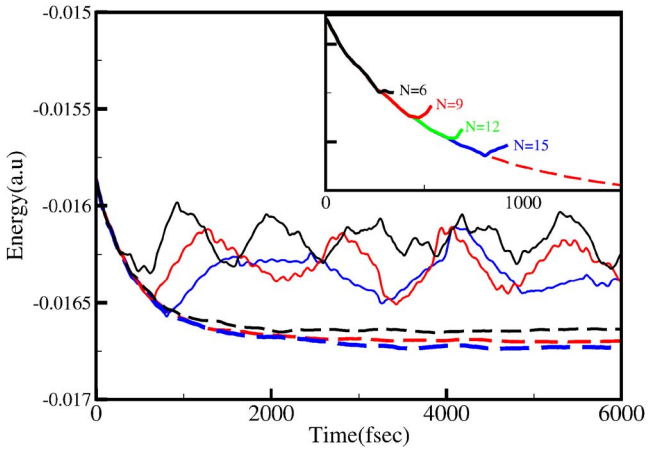


FIG. 3. (Color online) Decay of system energy as a function of time calculated by the surrogate Hamiltonian (solid) and stochastic surrogate Hamiltonian method (dashed) with increasing number of bath modes. The inset shows the short time dynamics up to 1500 fs; six bath modes are coded in black, nine bath modes in red, and 15 bath modes in blue.

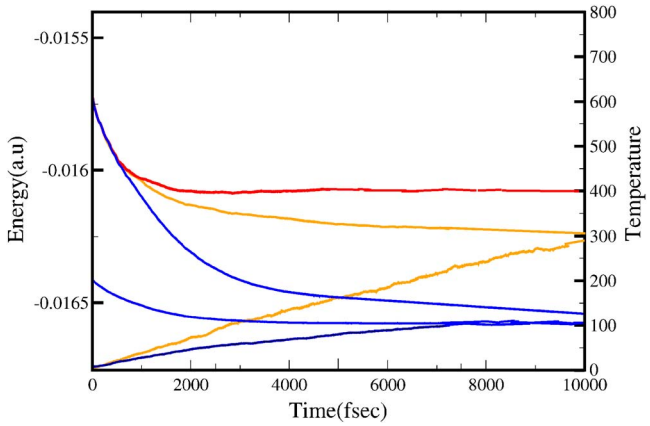


FIG. 5. (Color online) Approach to equilibrium of three initial system-bath correlated state corresponding to $T=0$ K, $T=200$ K, and $T=600$ K. Energy as a function of time for different secondary bath temperatures (400 K, 300 K, and 100 K). 15 primary bath modes are used for the calculation averaged over 24 realizations. The initial system-bath correlated thermal state was generated by the stochastic thermal wave function method (Ref. 19).

Hamiltonian shows an unphysical revival, which is absent in the stochastic surrogate Hamiltonian. A more detailed analysis of the convergence is displayed in Fig. 3, showing the decay of the primary system's energy with time. In the insert the typical convergence of the surrogate Hamiltonian method with increasing number of bath modes is shown; 15 bath modes were required to converge the results up to 500 fs. At this time artificial recurrence takes place, returning energy from the bath to the system. For longer times shown in the main part of Fig. 3, the surrogate Hamiltonian and stochastic surrogate Hamiltonian deviate. Only the stochastic surrogate Hamiltonian method is able to follow the dynamics to thermal equilibrium; the surrogate Hamiltonian method shows the unphysical oscillatory flow of energy from the bath back to the system.

The convergence of the stochastic surrogate Hamiltonian with respect to the number of stochastic realizations $K$ is shown in Fig. 4. As expected the standard deviation of any system variable $\sigma$ decreases as $1/\sqrt{K}$. The slope of this graph increases with the number of primary bath modes $N$ leading to the relation $\sigma \propto 1/\sqrt{K2^{N/2}}$. This suggest that half the modes of the primary bath participate in self-averaging.

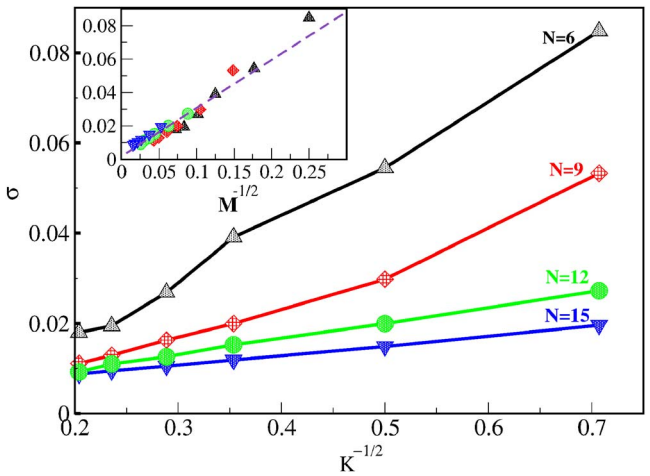


FIG. 4. (Color online) The standard deviation $\sigma$ of the variable $\int_{t_1}^{t_2}(\rho(0)\cdot\rho(t))dt$ as a function of $K^{-1/2}$, where $K$ is the number of realizations, for different numbers $N$ of bath modes. ($t_1=5750$ fs and $t_2=6000$ fs). The inset shows $\sigma$ as a function of $1/M^{1/2}$, where $M=K2^{N/2}$. The symbols correspond to the number of bath modes $N$ in the main plot.

The ability of the stochastic surrogate Hamiltonian method to simulate environments of different temperatures is shown in Fig. 5. Three correlated initial states of the system and primary bath were prepared at different temperatures using the random phase thermal wave packet method.[19] At $t=0$ the combined system-bath was coupled to the secondary stochastic bath at different temperatures. Reference states $\hat{\boldsymbol{\rho}}_S(T)$ at these temperatures were prepared using the random phase thermal wave packet method. As can be seen in Fig. 5 the combined system-bath relaxed to the new thermal equilibrium. It is clear that the final equilibrium state is independent of the initial state of the system. We found also that the overlap between the final state generated dynamically by the stochastic surrogate Hamiltonian $\hat{\boldsymbol{\rho}}_S(t=8000)$ and the reference state $\hat{\boldsymbol{\rho}}_S(T)$ was better than $(\hat{\boldsymbol{\rho}}_S(t=8000)\cdot\hat{\boldsymbol{\rho}}_S(T)) \leq 0.995$.

An important characteristic of system-bath dynamics is the ratio between energy relaxation and dephasing. Energy relaxation is always accompanied by dephasing. In the Markovian limit one obtains $T_2 \leq 2T_1$. This limit is achieved in the stochastic surrogate Hamiltonian when the rate of energy flow in and out of the primary bath is balanced $\Gamma_j=\lambda_j$. When the rate of the swap operation $\Gamma_j$ becomes larger than system-bath coupling term $\lambda_j$ pure dephasing overwhelms leading to $T_2 \ll 2T_1$. Figure 6 shows the change in the ratio $T_1/T_2$ as a function of $\Gamma_j/\lambda_j$, starting from the limit of $1/2$ dominated by energy relaxation and reaching the limit of pure dephasing when $\Gamma_j \gg \lambda_j$.

## IV. DISCUSSION

Quantum simulations are overwhelmed by the exponential growth in computation resources with the number of degrees of freedom. A converged quantum dynamical calculation that can simulate any possible observable is therefore

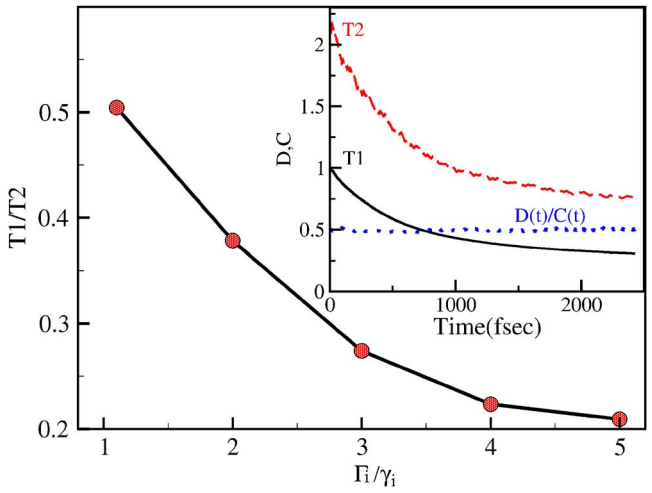


FIG. 6. (Color online) The ratio between energy relaxation ($T_1$) and dephasing ($T_2$) as a function of the ratio between the rates $\Gamma_j/\lambda_j$. The energy relaxation timescale $T_1$ is extracted from a fit to the relaxation of the diagonal elements of density operator $D(t)=\sqrt{\Sigma_j(\rho_{jj}(t)-\rho_{jj}(T))^2}$ in the energy representation. The dephasing timescale $T_2$ is extracted from decay of the off diagonal terms $C(t)=\sqrt{\Sigma_{i\neq j}\rho_{ij}^2}$. The inset shows the functions $D(t)$ and $C(t)$ and their ratio as a function of time.

severely limited. A constructive approach is to limit the goals of the simulation to a small number of preselected observables. The challenge is to develop an approach that can guarantee convergence for the observables of choice. In the present study we focus on the observables of a primary system coupled to a bath. The convergence can be related to the projection of the calculated state to the reference state defined by the scalar product $(\hat{\boldsymbol{\rho}}_S\cdot\hat{\boldsymbol{\rho}}_S^{\mathrm{ref}})$ of the reduced density operator. The basic idea of the surrogate Hamiltonian is that the bath can be mapped to an alternative one without influencing the primary observables. For example, we have shown that the spin bath converges to the results of a harmonic bath.[29]

The simplification of introducing the surrogate bath does not overcome the problem of the exponential growth in computational resources when the number of bath modes is increased to obtain convergence. The stochastic surrogate Hamiltonian overcomes the exponential growth by adding an infinite secondary bath, which eliminates this artificial recurrence. Formally we changed the dynamics from unitary to nonunitary described by open system Liouville dynamics.[6,8,9] As can be seen in Fig. 3 at short times the dynamics of the surrogate Hamiltonian and stochastic surrogate Hamiltonian coincide, while at longer times the infinite secondary bath eliminates recurrence. Convergence is reassured due to the fact that as the number of primary modes is increased, the coupling to the secondary bath decreases.

In order to maintain a wave function description of the state of system and primary bath, we chose to implement the open system dynamics by a stochastic method. Such methods have been shown to be completely equivalent to the Lindblad open system dynamics.[21–25,30] There is an infinite freedom in choosing the stochastic method. The methods based on the stochastic nonlinear Schrödinger equations are hard to implement in the large system-bath Hilbert space. We therefore chose to adopt the swap method of Gisin,[27] where the linear system-bath dynamics is maintained. Gisin has proven that a succession of swap operations drives a two-level primary system to thermal equilibrium. This property is sufficient for equilibrating the primary bath and eliminating recurrence. It is interesting to note that the swap operation that collapses a single bath mode only partially destroys the system-bath entanglement. The phenomenon is similar to the ability to store an electromagnetic field in a large ensemble of cold Rb atoms[31,32] when unavoidably single atoms are subject to decoherence by the environment.

The quantum stochastic methods should not be confused with the stochastic averaging in phases space in classical molecular dynamics.[33] Semiclassical methods naturally adopted the idea of stochastic averaging over phase space.[34] Surface hopping is conceptually closer to the stochastic swap procedure,[35,36] but it results in a complete system-bath loss of coherence.

The general convergence of any stochastic method scales as the square root of the number of realizations. The scaling factor depends on the variance of the observable. A small variance means very fast convergence. As can be seen in Fig. 4 the variance of the primary system observables is small. We find that this variance scales as the inverse square root of the number of states in half the bath modes. A similar phenomenon was found in the convergence of the random phase thermal wave function.[19] This behavior is an indication for self-averaging. We can speculate that its source is in the complex many body system-bath dynamics.

## V. SUMMARY

The new stochastic surrogate Hamiltonian is a significant step in the development of realistic system-bath simulations. In principle the surrogate Hamiltonian method converges to the true dynamics when the number of bath modes increases. The stochastic surrogate Hamiltonian is able to keep this characteristic without the exponential growth of computation resources with the simulation time. We find that a simulation with 12 bath modes corresponding to a Hilbert size of $\sim 2\times 10^5$ averaging 24 realizations is sufficient to simulate a complete thermal relaxation process. In comparison the standard surrogate Hamiltonian would not converge with 30 bath modes corresponding to a Hilbert size of $\sim 10^{12}$. The major advantage of the stochastic surrogate Hamiltonian is that each realization of the dynamics is unitary and linear. As a result the efficient propagation methods for quantum molecular dynamics can be employed.

## ACKNOWLEDGMENTS

We are grateful to the Ministry of Science in Niedersachsen and the Chemistry division of the NSF for support of this work. We want to thank Torsten Kluner and Lajos Diosi for helpful discussions.

[1] R. Kosloff, J. Phys. Chem. **92**, 2087 (1988).
[2] S. Borowski and T. Klüner, Chem. Phys. **304**, 51 (2004).
[3] G. J. Kroes, E. J. Barends, and R. C. Mowrey, Phys. Rev. Lett. **78**, 3583 (1997).
[4] R. Zwanzig, J. Stat. Phys. **9**, 215 (1973).
[5] T. Arimitsu, Y. Takahashi, and F. Shibata, Physica A **100**, 507 (1980).

[6] H.-P. Breuer and F. Petruccione, *Open Quantum Systems* (Oxford University Press, New York, 2002).
[7] E. B. Davies, Commun. Math. Phys. **39**, 91 (1974).
[8] G. Lindblad, Commun. Math. Phys. **48**, 119 (1976).
[9] V. Gorini, A. Kossokowski, and E. C. G. Sudarshan, J. Math. Phys. **17**, 821 (1976).
[10] R. Alicki and K. Lendi, *Quantum Dynamical Semigroups and Applications* (Springer-Verlag, Berlin, 1987).
[11] G. Ashkenazi, R. Kosloff, and M. A. Ratner, J. Am. Chem. Soc. **121**, 3386 (1999).
[12] M. Berman, R. Kosloff, and H. Tal-Ezer, J. Phys. A **25**, 1283 (1992).
[13] R. Kosloff, Annu. Rev. Phys. Chem. **45**, 145 (1994).
[14] W. Huisinga, L. Pesce, R. Kosloff, and P. Saalfrank, J. Chem. Phys. **110**, 5538 (1999).
[15] E. Geva, E. Rosenman, and D. Tannor, J. Chem. Phys. **113**, 1380 (2000).
[16] R. Baer and R. Kosloff, J. Chem. Phys. **106**, 8862 (1997).
[17] C. P. Koch, T. Kluner, and R. Kosloff, J. Chem. Phys. **116**, 7983 (2002).
[18] C. P. Koch, T. Klüner, H.-J. Freund, and R. Kosloff, Phys. Rev. Lett. **90**, 117601 (2003).
[19] D. Gelman and R. Kosloff, Chem. Phys. Lett. **129**, 381 (2003).
[20] E. Luc-Koenig, F. Masnou-Seeuws, and R. Kosloff, Phys. Rev. A **76**, 053415 (2007).
[21] N. Gisin, Phys. Rev. Lett. **52**, 1657 (1984).
[22] L. Diosi, Phys. Lett. A **129**, 419 (1988).
[23] J. Dalibard, Y. Kastin, and K. Molmer, Phys. Rev. Lett. **68**, 580 (1992).
[24] N. Gisin and I. C. Percival, J. Phys. A **25**, 5667 (1992).
[25] L. Diosi, N. Gisin, and W. T. Strunz, Phys. Rev. A **58**, 1699 (1998).
[26] D. Gelman, G. Katz, R. Kosloff, and M. A. Ratner, J. Chem. Phys. **123**, 134112 (2005).
[27] M. Ziman, P. Stelmachovic, V. Buzek, M. Hillery, V. Scarani, and N. Gisin, Phys. Rev. A **65**, 042105 (2002).
[28] M. Nest and H.-D. Meyer, J. Chem. Phys. **119**, 24 (2003).
[29] D. Gelman, C. P. Koch, and R. Kosloff, J. Chem. Phys. **121**, 661 (2004).
[30] O. V. Prezhdo, Phys. Rev. Lett. **85**, 4413 (2000).
[31] D. Phillips, A. Fleischhauer, A. Mair, R. Waslworth, and M. D. Lukin, Phys. Rev. Lett. **86**, 783 (2001).
[32] K. S. Choi, H. Deng, J. Laurat, and H. J. Kimble, Nature (London) **452**, 67 (2008).
[33] N. Metropolis, A. W. Rosenbluth, M. N. Rosenbluth, A. H. Teller, and E. Teller, J. Chem. Phys. **21**, 1087 (1953).
[34] S. X. Sun and W. H. Miller, J. Chem. Phys. **117**, 5522 (2002).
[35] J. C. Tully, J. Chem. Phys. **93**, 1061 (1990).
[36] F. J. Webster, J. Schnitker, M. S. Friedrichs, R. A. Friesner, and P. J. Rossky, Phys. Rev. Lett. **66**, 3172 (1991).